Link to publication

OPTIMISED BEAM DESIGN USING INNOVATIVE FABRIC-FORMED CONCRETE

J. Garbett[1], A. P. Darby[2,*] and T.J.Ibell[2]

[1]Buro Happold, Camden Mill, Lower Bristol Road, Bath, UK
[2]Department of Architecture and Civil Engineering, University of Bath, Bath, BA2 7AY, UK

Abstract: With pressure on designers to provide sustainability driven structural solutions, making best use of resources in structural design becomes paramount. In particular, cement is one of the greatest CO_2 contributors and its use in concrete structures means that optimisation to minimise material and weight is crucial. Optimal design techniques, such as the bone growth analogy, result in extraordinary images of curvaceous and interesting optimised systems. However, the link to practical construction has not always been considered. Simultaneous with this sort of optimisation, various researchers around the world have been looking at the use of flexible fabric formwork for the casting of interesting architectural concrete structures. This previous research has not fully made the link between beauty and precise prediction of final geometry. This paper describes recent research at the University of Bath, which has created a link between aesthetic appeal, structural optimisation, precise definition of final geometric form, and practicality of construction. The paper describes how optimally designed flexibly-formed concrete structural elements may be designed and constructed. It is shown that accurate prediction of final bulbous shapes is possible, that control of structural capacity at any section of the element is feasible, and that highly-aesthetic outcomes are achievable.

Key words: fabric formwork, optimisation, reinforced concrete.

* Corresponding author: Dr Antony Darby, Department of Architecture and Civil Engineering, University of Bath, Bath, BA2 7AY, UK, email absapd@bath.ac.uk, Tel +44 1225 383182, Fax +44 1225 386691

1. INTRODUCTION

In recent years methods for flexibly forming concrete beams have been developed, most notably by the architect Mark West of the University of Manitoba, Canada (West (2001), West (2005), West (2006)). This forming method uses hung fabric formwork, which will take a predictable shape when filled with concrete and allows variable section beams to be easily formed at reasonably low costs. This presents designers with the opportunity to develop fully optimised concrete elements, such as beams, where the section varies throughout the member length in response to likely loading. The optimised beam provides structural efficiency whilst minimising materials to produce a structurally and architecturally elegant form. Structural optimisation has always been an ultimate goal in engineering and as the focus on sustainable design grows ever stronger, the need for optimised structures, which use the minimum amount of material possible, also grows. Although structural optimisation has been the subject of much research, very few studies have combined structural optimisation with practical fabrication methods.

The question, then, is how this shape should be optimised given construction constraints. One particularly attractive method of optimising concrete structures is through a bone growth analogy where areas of material under high levels of stress grow and areas of low stress decay. In this way, over time, bones become highly optimised so that all the material in the structure becomes equally stressed. A number of studies have applied the bone growth analogy to structural optimisation with varying degrees of success. Xie and Steven (1993) proposed a simple evolutionary procedure for the shape optimisation of structures, which took inspiration from the evolution of naturally occurring structures such as bone. Christie, Bettes and Bull (1998) developed the process further allowing material to be added and removed from the evolving shape. In addition the designer is given control of where material is added or removed allowing the creation of shapes which are practical for construction. The main drawback with this designer input, however, is that the most optimal shape is unlikely to be reached. Shave (2000) considered a different approach to the bone growth analogy, by optimising structures through 'adaptive remodelling' to minimise weight. The method starts from an initial form, defined by nodes around the section perimeter, which then move relative to the amount of stress at each point. This process creates a final shape with a relatively constant state of stress across the

section and has the advantage of allowing growth and decay whilst allowing designer input by allowing fixed nodes.

However, all these studies use the Von Mises stress as the stress criterion for adding or removing material. This works well for continuous isotropic materials such as steel and aluminium, but is not an appropriate model for concrete. The non-linear material properties and structural behaviour of reinforced concrete are much more complicated. Reinforced concrete involves two materials and it is assumed that concrete does not carry tension. Therefore a simplified optimisation approach is more appropriate, where sections along a beam are optimised to minimise weight whilst providing adequate capacity for the shear and flexure acting at the particular location.

Whilst structural optimisation has developed from early trial and error procedures through to modern numerical techniques, there is still a separation between theoretical optimisation and final products, which must be cost effective and easy to build. Christie, Bettess and Bull (1998) raise the point that although a large amount of information is written on structural optimisation, very little has been published on its practical application. With the development of flexible fabric formwork, the possibility of commercially viable, optimised concrete structures is much nearer to being realised.

2. FABRIC FORMWORK

Although fabric formwork has existed for many years it was not until the 1960's that the technology really took off, with the introduction of low cost, high strength and highly durable synthetic fibres (Lamberton, 1989). However in the past fifteen years or so the architectural possibilities of flexibly forming concrete have begun to be exploited, most notably with the work of Mark West at the University of Manitoba and Kenzo Unno, a Tokyo based architect (West, 2005). Interest is now spreading internationally with research taking place at a number of universities. There has been a big interest in this technology from an architectural perspective, but there is still a wealth of structural possibilities yet to be investigated. In particular, fabric formwork provides the means of easily forming more complex optimised components and therefore creating significant material savings. Additionally, West (2005) argues that fabric

formwork itself is cheaper and requires significantly less material and labour compared to traditional timber and steel formwork.   Furthermore, fabric formed concrete can offer a significant technical advantage over conventionally cast concrete. Excess vehicle water in the concrete is allowed to escape from the formed surface which significantly improves the mechanical properties of the concrete and allows highly workable concrete mixes to be used, while still providing a low final water-cement ratio (Ghaib and Gorski, 2001). In addition 'case hardening' occurs at the surface due to the low water-cement ratio, which creates a very fine surface finish, removing the need for further surface treatment (West, 2005).

For construction of beams, the simplest forming technique uses a 'U-shaped' timber forming-table, on to which fabric is attached and hung or draped into the central space. Reinforcement is laid into the fabric which is then filled with concrete, forming a hydrostatic shape. This fabric formed beam provides a potential means of forming more complex optimised components and therefore creating significant material savings. However, if this is to be realised, design methods must be provided to allow this optimal shape to be defined within the constraints of the forming technique. The aim, therefore, of the work presented in this paper, is to develop simple form-finding and optimisation procedures for concrete beams which can be practically constructed using fabric formwork. Tests on such optimised specimens have been carried out to demonstrate the practicality of their construction and behaviour.

3. FORM-FINDING THE HYDROSTATIC SHAPE

When concrete is poured into a hung fabric mould, the resulting shape has a predictable hydrostatic form. To be able to effectively design simply hung flexibly-formed beams the basic parameters of this hydrostatic form must be known. Work was carried out at the University of Bath (Ibell *et al.,* 2007) to find equations that relate the top breadth, *b*, and depth of the hung shape, *d*, to the required fabric perimeter, *P*, and the cross-sectional area, *A,* as shown in Figure 1 (Bailiss, 2006). Through careful measurements on test sections, using different top breadths and varying lengths of fabric the following empirical relationships can be derived.

$$P = \frac{-(0.212b-d) \pm \sqrt{(0.212b-d)^2 - 4 \times 0.396 \times (-0.49b^2)}}{2 \times 0.396}$$

(1)

$$A = \left[\left(\frac{\left(\frac{b}{P}\right) - 0.05}{0.65} \right)^{-0.3} - 0.34 \right] \times (b \times d) \qquad (2)$$

These findings allow accurate fabrication of beams to a defined depth and top breadth. However the equations do not give any real description of the final hydrostatic shape. This is an issue in terms of optimisation, since, while the total area of material is known, it is not known where this material is located within the section. Therefore, the physical study carried out by Bailiss (2006) was investigated further and equations for the *maximum* width of the section, *w*, and the location of this maximum within the section depth, *h*, (as indicated in Figure 1) were determined by plotting the breadth ratio (*w/b*) and the depth ratio (*h/d*) against the section breadth to depth ratio (*b/d*). The following empirical relationships were derived:

$$w = \left(3.2016 \times \left(\frac{b}{d}\right)^2 - 5.7721 \times \left(\frac{b}{d}\right) + 3.6111 \right) \times b \qquad (3)$$

$$h = \left(-0.3263 \times \left(\frac{b}{d}\right) + 0.6659 \right) \times d \qquad (4)$$

Equations 1-4 allow the cross section of a fabric formed beam to be defined, thus providing a basis for optimisation procedures.

4. BEAM OPTIMISATION

A series of beams were developed using an optimisation procedure based upon minimising use of material whilst adequately carrying the load at any section, subject to the practical limitations presented by construction techniques. This practical construction element of the procedure is crucial in terms of producing buildable and economically viable structures. The fabric formwork construction technique opens up such possibilities.

However, the fabric forming process, although very versatile, still imposes a number of constraints upon the optimisation process. For simply hung sections, the hydrostatic form can be calculated through the shape functions given by Eqns 1-4. The applicability of these equations is limited by the extent of the original study upon which they are based. Therefore the top breadth must be greater than 10% of the fabric perimeter (*b/P* > 0.1) and the cross-sectional area must be

greater than 10% of the top breadth multiplied by the section depth (i.e. $A/(b*d) > 0.1$). For top breadth and section depth a minimum must be set to control what can physically be built and a maximum also set to control the stability of the shape. Furthermore, for the purposes of fabricating test specimens, the following parameters were assumed:

- 8mm reinforcement was used to allow the bars to be bent easily.
- The only reinforcing steel in the section was a single bottom tension steel bar for ease of construction. This was mainly due to the difficulty of accurately positioning any other reinforcing steel.
- The concrete cover to reinforcement was taken as 30mm.

Optimisation can only be achieved for a specific envelope of loading on a beam. However, for the purposes of demonstrating the technique, the beam was designed purely to carry a uniformly distributed load. This allowed a smooth beam geometry to be generated. Providing such a load in practice was difficult so the uniform load was approximated by 5-point loading with an ultimate total design load of 15kN.

The optimisation procedure was gradually developed as constraints were added or removed. This allowed optimal development to be considered alongside the physical method of flexibly forming each beam. The starting point for the optimisation was a standard reference rectangular beam (Figure 2a) which was found to require a cross section of 100mm wide x 253mm deep(a total beam volume of 0.0506m^3). The next stage was a flexibly formed beam with constant top breadth but varying depth along its length (Figure 2b). Further optimisation was achieved by allowing the top breadth to vary (Figure 2c). The form of these beams was dictated by the hydrostatic shape, which limited the amount of optimisation that could be achieved. Therefore the final stage allowed variation of this cross-section along the beam length, to further optimise the use of material in each section. For each beam, the length was divided at 100mm centres so that the unique cross-section at each position along the beam length could be defined according to the shear force and bending moment. This also assisted with setting out of the fabric when constructing the beams.

4.1. Constant top breadth – flexibly formed beam

The optimisation program was developed by initially considering a flexible fabric formed beam with a constant top breadth. Although this beam was not constructed, it allowed the concrete design theory to be developed. A constant top breadth of 100mm was specified (Figure 2b).

4.1.1. Optimisation for bending moment

Concrete design was based on BS8110 (British Standards Institution, 1997), a limit state design code which assumes that plane sections remain plane, that the concrete cannot carry tension and that the stress distribution in the concrete above the neutral axis is approximately parabolic. This stress distribution is approximated by an equivalent rectangular stress block, simplifying the design equations, particularly appropriate in the case of non-rectangular cross-sections (Mosley, *et al*., 1999).

It is assumed that, throughout the beam length, rather than just at the position of maximum moment, the steel yields before the concrete crushes, providing a ductile failure mode. Due to the constraint, in this example, of a constant width at the top of the beam, the only parameter which can be varied is the depth, *d*, which is directly linked to the fabric perimeter.

For equilibrium the force in the concrete must equal the force in the steel, $F_c = F_s$. Considering a simplified rectangular stress block and, assuming the concrete in compression to be approximately constant in width, *b*, (since it is likely to be a relatively shallow region), gives the force in the concrete as:

$$F_c = 0.67 f_{cu} \times 0.9 x \times b \tag{5}$$

where f_{cu} is the characteristic concrete cube strength. Hence, rearranging Eqn 5 the neutral axis depth, *x*, is given by:

$$x = \frac{F_c}{0.67 f_{cu} \times 0.9 \times b} \tag{6}$$

This is constant throughout the beam length since the concrete compression force must be constant to balance the steel force at yield. Therefore, it is only the lever arm, *z*, between the steel/concrete force couple which changes, in relation to the bending moment, *M*, experienced at each section along the beam, as defined by the loading:

$$z = \frac{M}{F_s} \quad\quad (7)$$

Hence, the total depth of the section, *d*, can then be calculated for this case as.

$$d = 0.45x + z + \left(\frac{\text{Ø}}{2}\right) + c \quad\quad (8)$$

Where *ø* is the bar diameter and *c* is the concrete cover.

Finally, substituting for *x* and *z* with Eqns 6 and 7 gives:

$$d = \left(\frac{0.45F_c}{0.67 f_{cu} \times 0.9 \times b}\right) + \left(\frac{M}{F_s}\right) + \left(\frac{\text{Ø}}{2}\right) + c \quad\quad (9)$$

The designer can use Eqn 9 directly to find the required depth at any point along the section due to bending moment.

4.1.2. Optimisation for shear

The beam must also be able to carry shear at any point. In a fully optimised section the shear capacity and bending capacity would be met simultaneously, although in reality it would be sensible to provide a higher moment capacity to prevent the possibility of brittle shear failure. To allow for practicalities of construction the beam is designed without shear reinforcement. It is also assumed that any inclined tension steel does not add to the shear capacity of the section, although in reality there will be a small effect. Shear behaviour in concrete is very complicated particularly with the absence of shear stirrups. However, adopting the empirical shear analysis approach from BS 8110, the shear strength of the concrete is given as:

$$v_c = 0.79\left(\frac{100A_s}{b.d'}\right)^{1/3}\left(\frac{400}{d'}\right)^{1/4}\left(\frac{f_{cu}}{25}\right)^{1/3}\left(\frac{2d'}{a_v}\right) \quad\quad (10)$$

Where d' is the effective depth of the section, A_s is the area of tension steel and a_v is the shear span. The shear stress at any section is:

$$v = \frac{V}{b.d'} \quad\quad (11)$$

By equating Eqns 10 and 11 an equation for the effective depth, d' can be produced:

$$d' = \left(\frac{V}{0.79b \left(\frac{100A_s}{b} \right)^{1/3} (400)^{1/4} \left(\frac{f_{cu}}{25} \right)^{1/3}} \right)^{12/5}$$

(12)

This equation does not take account of the shear enhancement effect close to the supports, which, if included, results in an implicit equation, requiring an iterative solution. However, given that the section is ideally shallow near supports (due to low moment) arching action will be negligible. Therefore, neglecting this, Eqn 12 gives the effective depth of the section and is applicable as long as the constraints laid out in BS8110-1:1997 Table 3.8 are followed.

Additionally, for later use, an equation in terms of the top breadth, b can also be found:

$$b = \left(\frac{V}{0.79d \left(\frac{100A_s}{d'} \right)^{1/3} \left(\frac{400}{d'} \right)^{1/4} \left(\frac{f_{cu}}{25} \right)^{1/3} \left(\frac{2d_1}{a_v} \right)} \right)^{3/2}$$

(13)

In order to take into account the irregular shape of the hydrostatic section, some form of shape correction factor is necessary. For moment calculations it can be assumed that the effective breadth is equal to the top breadth, i.e. it is unaffected by shape since only the top compression region contributes to the moment capacity. However, for shear capacity where the full depth of the cross section contributes to the shear strength, an effective breadth of the section must be used rather than the width at the top, b. This in turn is related to the top breadth and depth of the section. As a pragmatic simplification, based upon further studies of the cross section analysis carried out by Bailiss (2006), the value suggested is to use $b=0.9w$ in Eqn 12 where w is the maximum breadth of the section as defined by Eqn 3. This is an approximation since this breadth varies throughout the section depth, but allows the capacity to be controlled without overestimation.

The resulting beam, based on optimising the depth for shear and flexure along the beam length, resulted in a reduction in the volume of concrete used of 15%, compared with the reference rectangular beam.

4.2 Varying top breadth (Beam 1)

To allow for further optimisation of the form, the width of the top of the beam was allowed to be adjusted (Figure 2c). This beam was fully developed from the optimisation stage through to construction and testing and is referred to as Beam 1. Each section was again optimised for moment and shear along the beam. However, in this case; optimisation was achieved through minimising the section area, A, rather than merely optimising section depth. A minimum limit on the top breadth was set at 60mm, as a construction constraint, allowing the concrete to be poured and compacted by hand. For each section, Eqns 9 and 12 were for used depth, d, together with iteration of all possibilities of breadth, b, in order to find the smallest cross-sectional area, given by Eqn 2.

Figure 3 shows how the section develops as it goes through each stage of the optimisation process. Due to symmetry the program only analyses half the beam. The minimum allowable section depth was set to 50mm and this constrains the depth when the beam is only optimised for moment (Figure 3a). Once shear is introduced the most obvious effect is the increase in depth at the ends of the beam (Figure 3b). This provides the optimum shape to carry 5 point loading and is then smoothed to improve aesthetics (Figure 3c). Towards the centre of the beam the moment is relatively large but the shear small. Therefore to minimise the section area the top breadth reduces as much as possible (Figure 3d). This is because the depth of the section required for flexural optimisation does not vary very much with changes in the top breadth (since the main governing criteria is the lever arm, z, which is not affected by the top breadth, given the small neutral axis depth). The reduction in the final top breadth is limited to 62mm, due to the fact that the top breadth cannot be less than 10% of the fabric perimeter, in order to comply with the empirical formulae.

The resulting optimised shape of the beam can be seen as a 3D model in Figure 4. Compared with the reference rectangular beam, the volume of concrete is 25% less, representing an

additional saving of 10% compared with the constant top breadth beam. However, this is just as capable of carrying the required loading. The moment capacity is slightly higher than required at the ends, where shear is more dominant whilst, near the centre, the shear capacity is much higher than needed, due to an excess of concrete within the tension zone below the neutral axis as the fabric cross section bulges out when taking on the hydrostatic form. This highlights a problem in this forming method, where a purely hydrostatic form is created.

4.3. 'Keyhole' shaped section (Beam 2)

To improve the optimisation of the material within each section, it was considered that a beam could be fabricated with a central hollow section as shown in Figure 2d. This hollow area could then be optimised to minimise the amount of unstressed concrete below the neutral axis in each section. Whilst this could perhaps be constructed using, for instance a hollow or lightweight former, it was not seen as a practical construction method and would be difficult to accurately construct. Therefore, the second beam to be developed used a solid 'keyhole' shape as shown in Figure 2e, which allowed each section to be more highly optimised, but aimed at keeping construction, materials and labour requirement, relatively low. This beam was referred to as Beam 2 and the optimised form was developed alongside the construction technique. The proposed construction technique was to apply two timber formers wither side of the fabric to form a variable depth and width web section.

Since most of the section was no longer constrained by the hydrostatic form, a significant change in approach was required in the development of the optimisation procedure. Instead of being optimised to achieve the minimum possible area, the section was now optimised to the minimum dimensions required to carry the moment and coexistent shear. Large amounts of under-stressed material below the neutral axis could be removed.

Again each section was optimised for moment and shear using BS8110 as a basis for design. Firstly considering moment, the section was optimised using Eqns 6 and 9. As there is a continuous reinforcing bar running along the length of the beam, the force in the steel at yield, F_s, is constant along the length of the beam. Therefore, since $F_c = F_s$ the top compression region must also be constant in size along the entire length of the beam. The dimensions of this 'flange'

region are found using either a specified depth or width of flange. In normal design it is likely that the flange width would be specified and so the top breadth was taken as 100mm. The resulting flange depth represents the depth of the neutral axis and any concrete below this depth is assumed to be ineffective in terms of adding to flexural capacity. The required section depth due to moment can then be calculated from Eqn 9.

The section can then be optimised for shear, using Eqns 12 and 13. Towards the centre of the beam this optimisation simply finds the necessary width of web for the section depth. To allow for concrete compaction between the web formers, the minimum web width was limited to 30mm. Moving away from the centre of the beam, shear increases and the depth decreases (governed by moment), requiring that the web width increases. A smooth curve was derived from the optimisation output to vary the width of web along the length of the beam. This allowed the use of curved web formers for ease of construction. A 'bulb' was allowed to form at the bottom of the section, around the steel, to allow sufficient concrete cover to the steel. Towards the ends of the beam the section shape again became controlled by the hydrostatic form since the depth was insufficient to introduce a web former. Figure 5 shows the final shape as optimised.

Compared with the hydrostatic shape, there is little change in moment capacity along the section, but the shear capacity is much closer to the required capacity. The resulting beam volume after the optimisation process represents a 55% material saving from the standard rectangular section and an additional 40% material saving from Beam 1. This shows that the optimisation process has been successful in reducing the amount of material below the neutral axis, even within the construction constraints.

5. BEAM FABRICATION

Once the sizes and design parameters of Beams 1 and 2 had been established by the optimisation procedures, both beams were constructed. This allowed the associated construction techniques to be assessed and the beams to be tested. This in turn meant that the practicality of the design and success of the optimisation process could be assessed.

A forming table consisted of 'U' shaped MDF ribs, which were connected by timber stringers at the corner points as shown in Figure 6(a). Access was allowed underneath the table to vibrate the

beams during pouring and to fix the web formers in place during the fabrication of Beam 2. The tabletop could be altered to provide the required profile at the top of the beam.

A heavyweight 12oz furniture hessian was used as the fabric formwork for all beams. The fabric was marked out and fixed at the edge of the tabletop. The edge of the fabric was then lapped around a 3mm diameter bar and fixed down to the tabletop to ensure that the fabric hung evenly. Steel end plates (Figure 6(b)) were fitted at each end of the beam and bolted to the forming table, fixing the fabric in position. These plates provided ends to the formwork and also allowed the reinforcement to be welded into position. The 8mm diameter reinforcing bar was pre-bent around a jig to the required profile and welded in place. Strain gauges were fitted to the reinforcing bar at five positions along its length (near each end, in the middle and at quarter points). The concrete mix was designed to ensure a workable consistency and to take into account the bleeding of excess water through the fabric, resulting in a characteristic cube strength of 30N/mm^2. The concrete was mixed and then added to the fabric mould in layers. After each layer the concrete was compacted and vibrated from below to ensure good compaction and ensure the required shape was taken. The beam was left to cure before it was unbolted from the forming table and the hessian stripped from the beam.

For Beam 2, the process was modified to allow a web former to be placed. First, a small amount of concrete was added around the rebar and then the curved web formers were fitted into position (shown diagrammatically in Figure 6(c)). The rest of the concrete was then added in layers and vibrated and compacted as for Beam 1.

In both cases, the hessian sheared well into the required doubly curved shape. A significant amount of excess water escaped through the fabric during pouring. The constructed beam dimensions were measured and the final hydrostatic form was found generally to be similar to that predicted. The ends of the beam, however, were found to be slightly shallower than expected, due to a fabrication error. This has a large effect on the beam capacity as it reduces both the effective breadth, w, and depth, d, of the section. For Beam 2, the main problem encountered with the forming process was that the web formers were not sufficiently stiff so that the width of the web was generally greater than designed. Whilst this is not a problem in terms of beam capacity, it does affect the optimality of the beam in terms of material used. Furthermore,

the actual measured cube strength was found to be 35N/mm^2 at the time of testing, 5N/mm^2 more than used for design. Therefore, due to these minor changes in geometry and cube strength, the capacity of each beam was recalculated. Beam 1 was found to have a reduced predicted capacity of 14kN while, for Beam 2, an increased capacity of 18kN was predicted.

6. BEAM TESTING

6.1. Test set-up

Each beam was subjected to five-point loading and was simply supported with a pin at one end and a roller support at the other. The beam was loaded with three jacks, one in the middle and one at each quarter point. All jacks were hydraulically connected to one hand pump, to ensure an even load distribution. Load cells were connected to the bottom of each jack, to measure the applied load together with displacement transducers to measure corresponding deflections. The same instrumentation was used for both beams and the general set up is shown in Figure 7.

Each beam was gradually loaded and any cracking was monitored and marked on the beam at 0.5kN load increments. Both beams were loaded up until failure and a computer logged all loads, displacements and strains at 0.5 second intervals.

6.2 Test results – Beam 1

Cracks were first observed around 7.5kN near the beam supports (in the region which was found to be too shallow). As the loading was increased cracks continued to form all along the beam, towards the centre, and cracks continued to grow until a total load of about 10kN. At this point it was noted that cracking was reasonably evenly distributed and symmetrical along the entire length of the beam, indicating uniform stress. However, from this load onwards a crack near the roller support became dominant. This crack continued to grow towards the support and up to the top of the beam until the total loading reached about 12kN. As further load was applied, the crack then extended towards the left-hand jack and a shear failure occurred at just over 12.5kN. This compares with the predicted shear failure capacity of 14kN.

Figure 8 shows the variation in strain in the reinforcement with changes in load over the duration of the test. It can be seen that, for strain gauge 1, near the end where cracks were first observed, the strain increased suddenly at a load of about 4.5kN, indicating cracking may have occurred in this location earlier than observed. By the time the load reached about 9.5kN, strains had increased in all measured locations, indicating that cracking had spread along the beam. As the load was increased, significant flexural cracking began to occur in the centre of the section, as clearly shown by the rapid increase in strain at position 3 at a load of about 10.5kN suggesting the onset of ductile flexural behaviour at the centre of the beam. Unfortunately due to the weakness of the section towards the roller support, the capacity of the rest of the beam was not fully mobilised before brittle shear failure occurred at around 12.5kN. Strains increased towards about 2000 microstrain except for the two strain gauges 4 and 5, at the opposite end of the beam to the final failure, demonstrating the dominance of the crack at the position of strain gauge 1. Figure 9 shows the load deflection response for this beam.

6.3   Test results – Beam 2

The results of the Beam 2 test are shown in Figures 10 (load versus strain) and 11 (load versus central displacement). Cracks were first observed near the centre of the beam. As can be seen in Figure 10, the strain at position 3 immediately increased at the start of the test, more rapidlywhen the first cracks observed at the centre of the beam at about 6kN. This strain continued to increase as more load was applied. However, flexural cracks also began to form along the length of the beam and this is seen with the increase in strain at positions 2, 4and 5 at about 7.5kN. By a load of 18kN the central crack had opened up significantly, indicated by large strains in strain gauge 3, demonstrating ductile flexural behaviour. However, as the loading was further increased, sudden development of a shear crack near the left hand roller support, resulted in brittle failure at a load of 21kN. This compares with a predicted flexural capacity of 18kN.

6.4 Summary of beam tests

Beam 1 had a lower capacity than the original design due to the reduction in depth at the end of the constructed beam. Beam 2 had an increased capacity from the original design, due to increased web thickness from that designed. However, both beams failed through shear. This is due to the sensitivity of shear to structural errors, when no stirrups are included, and the

assumptions made in design. It would therefore be prudent to ensure that the design precludes brittle shear failure prior to flexural failure, although this will clearly be a sub-optimal design. Although Beam 2 had a higher capacity than beam 1, it used significantly less material than the purely hydrostatically fabric-formed beam. This demonstrates clearly the improved optimisation achieved. For both beams flexural cracks developed along the entire beam length, demonstrating an approximately constant flexural capacity along the beam length, which indicates that the flexural capacity relates well to the load distribution.

The difference in ductility between the two beams can also be seen in the relative amount of deflection at the centre. Beam 2 deflected by over 20mm at the centre before failure, while Beam 1 only deflected by just over 6mm. In Beam 1 the behaviour was completely dictated by the section where shear failure occurred. However, in Beam 2, failure began to occur along the length of the beam, as all sections began to reach their maximum flexural capacity and this resulted in a much more ductile failure, allowing greater deflections to occur.

These differences in ductility were mainly due to the fabrication error in Beam 1, resulting in premature shear failure near the shallow beam ends. Conversely, for Beam 2, the increased web size, compared to that designed for shear capacity, allowed significant yielding of the reinforcement to occur before shear failure occurred. Once beam capacities were recalculated to take into account the as-fabricated beam geometry, predicted capacities were reasonably accurate. This shows that if the correct geometry is formed the structural behaviour can be accurately predicted.

7. CONCLUSIONS

The main aim of this study was to combine structural optimisation with a practical fabrication process using a novel fabric forming technique. Two beams were optimised within the constraints of the construction processes with which they were then built. The final beams have shown that high levels of optimisation can be achieved with significant material savings. Compared with a conventional rectangular beam, the reduction in the quantity of concrete resulting from a simply designed and constructed fabric formed beam was 25%. For a more fully

optimised fabric formed beam, using additional web formers a 55% concrete saving was achieved.

Whilst the bone growth analogy cannot be directly applied to reinforced concrete, since it is not a uniform material and the shear behaviour is especially complicated, by using appropriate limit design criteria from BS 8110 the concrete section can be optimised for the coexistent moment and shear at each section along the beam. This optimisation is limited to a certain extent by the hydrostatic shape of a fabric formed beam but, by adding web formers into the construction process, optimisation of the material within each section is easier to achieve. However, complete optimisation will inevitably be limited by construction constraints.

Equations were produced to predict the hydrostatic form of a fabric formed beam and, compared to the measured as-built beam, were found to be reasonably accurate. This allows design to be carried out using predicted dimensions of the section and also allows 3D images to be produced allowing aesthetics to be judged. The design equations were also essential for calculating the perimeter of the fabric forming material along the beam length, required for the purposes of construction.

The ultimate load capacity of the two tested beams was shown to be fairly close to the predicted behaviour, using as-built parameters, although it varied from the optimally designed behaviour due to construction errors. Differences in capacity may also be due, in some part, to the difficulty of accurately positioning the reinforcement in a flexible fabric formwork. However, in general, the optimisation process was successful, since the theoretical output could be translated to a physical beam and its structural behaviour predicted.

Commercially the beneficial effect of increased optimisation is only effective if the amount of labour is not significantly increased. The simply hung beams are very effective in these terms, as reasonable levels of optimisation were achieved, while construction was quick and simple with minimal formwork. The introduction of web formers introduced additional complexity to the construction process but this is offset by the considerable material savings that can be achieved. Thus, flexible fabric formwork offers a new freedom of form and this huge potential can be

exploited to create concrete beams which are highly optimised, innovative and beautiful. Beams using the technique can also be built quickly and easily and behave in a predictable way.

REFERENCES

Bailiss. J. (2006). *Fabric formed concrete beams*. MEng dissertation, University of Bath, Bath, UK.

British Standards Institution, (1997). *BS 8110-1:1997 Structural use of concrete. Code of practice for design and construction.* UK, 168 pp.

Christie. W.C., Bettes. P. and Bull. J.W. (1998). *Self-designing structures: a practical approach.* Engineering Computations, Vol. 15 No. 1, pp.35-48.

Ghaib, M.A.A. and Gorski, J. (2001). *Mechanical Properties of Concrete Cast in Fabric Formworks*. Cement and Concrete Research, 31, pp. 1459-1465.

Ibell, T. J., Darby, A. P. and Bailiss, J. (2007). *Fabric-formed concrete beams*. Advanced Composites in Construction, University of Bath, Bath, 2-4 April 2007.

Lamberton. B.A. (1989). *Fabric Forms for Concrete.* Concrete International, December, pp.59-67.

Mosley, W.H., Bungey, J.H. and Hulse, R. (1999). *Reinforced Concrete Design.* Basingstoke : Palgrave.

Shave, J.D. (2000). *Optimised structural design by Adaptive Remodelling.* Technical Report, PB Kennedy & Donkin, Bristol, UK.

West, M. (2001). *Fabric Formed Concrete Structures*. First International Conference on Concrete and Development C and D 1, pp.133-142.

West, M. (2005). *A Brief Description of Fabric-Formed Concrete* [online]. Available from: http://www.umanitoba.ca/faculties/architecture/cast/CASTonline.html [Accessed Nov 2007]

West, M. (2006). *Flexible fabric molds for precast trusses.* Betonwerk und Fertigteil-Technik/Concrete Precasting Plant and Technology, v 72, n 10, 2006, p 46-52

Xie. Y.M. and Steven. G.P. (1993). *A Simple Evolutionary Procedure for Structural Optimisation.* Computers and Structures, Vol. 49 No.5, pp.885-96.
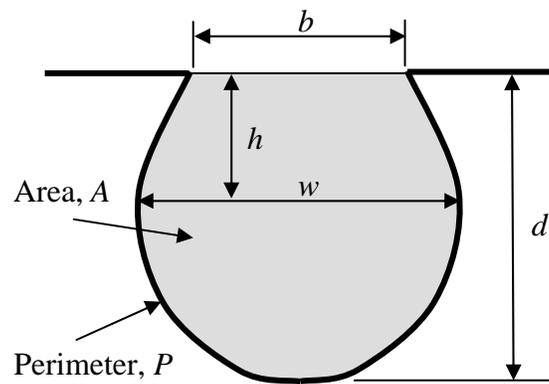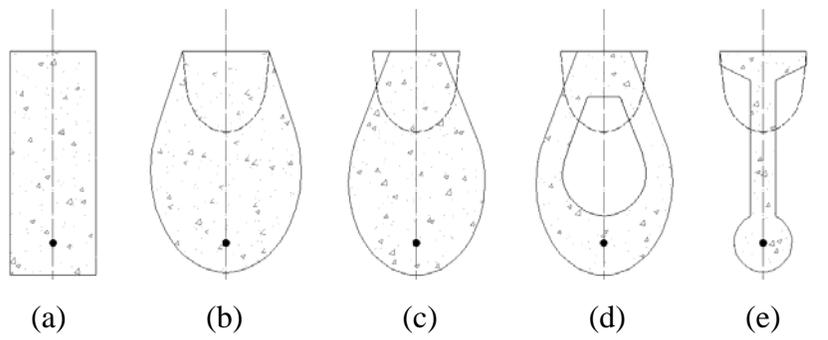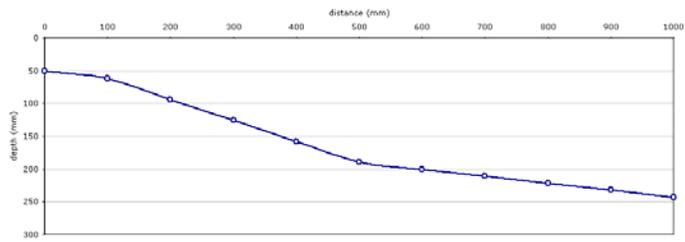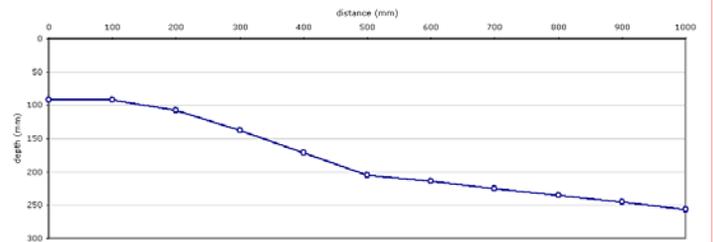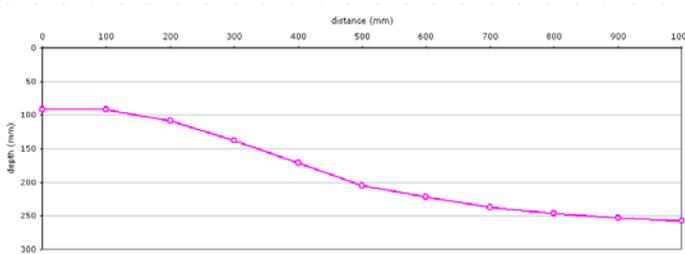
Figure 1: Cross section analysis

Figure 2: Evolution of optimal design process using fabric formed beams
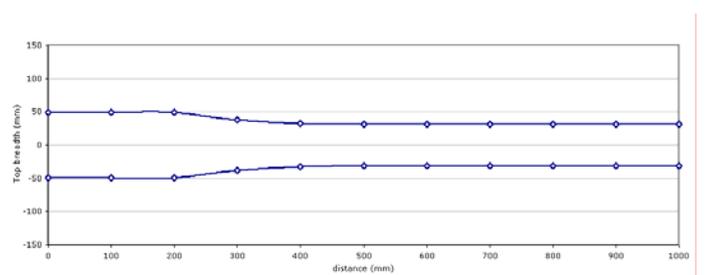
(a) Variation in depth due to moment along the beam.

(b) Variation in depth due to moment and shear along the beam.

(c) Adjusted depth profile to provide smooth shape for aesthetics.

(d) Final optimised top breadth

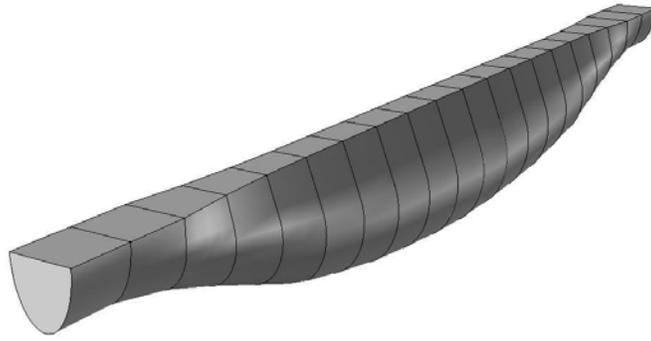Figure 3: Development of beam dimensions during optimisation

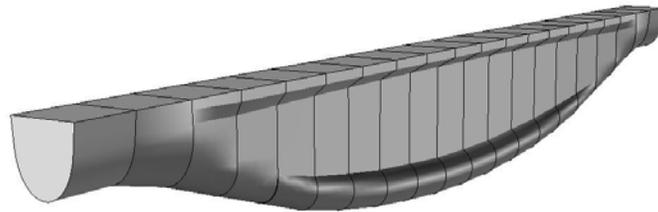Figure 4: Beam 1, optimally designed

Figure 5: Beam 2, optimally designed using web formers

(a)   (b)   (c)

Figure 6: Forming process: (a) forming table, (b) end plates, (c) web formers
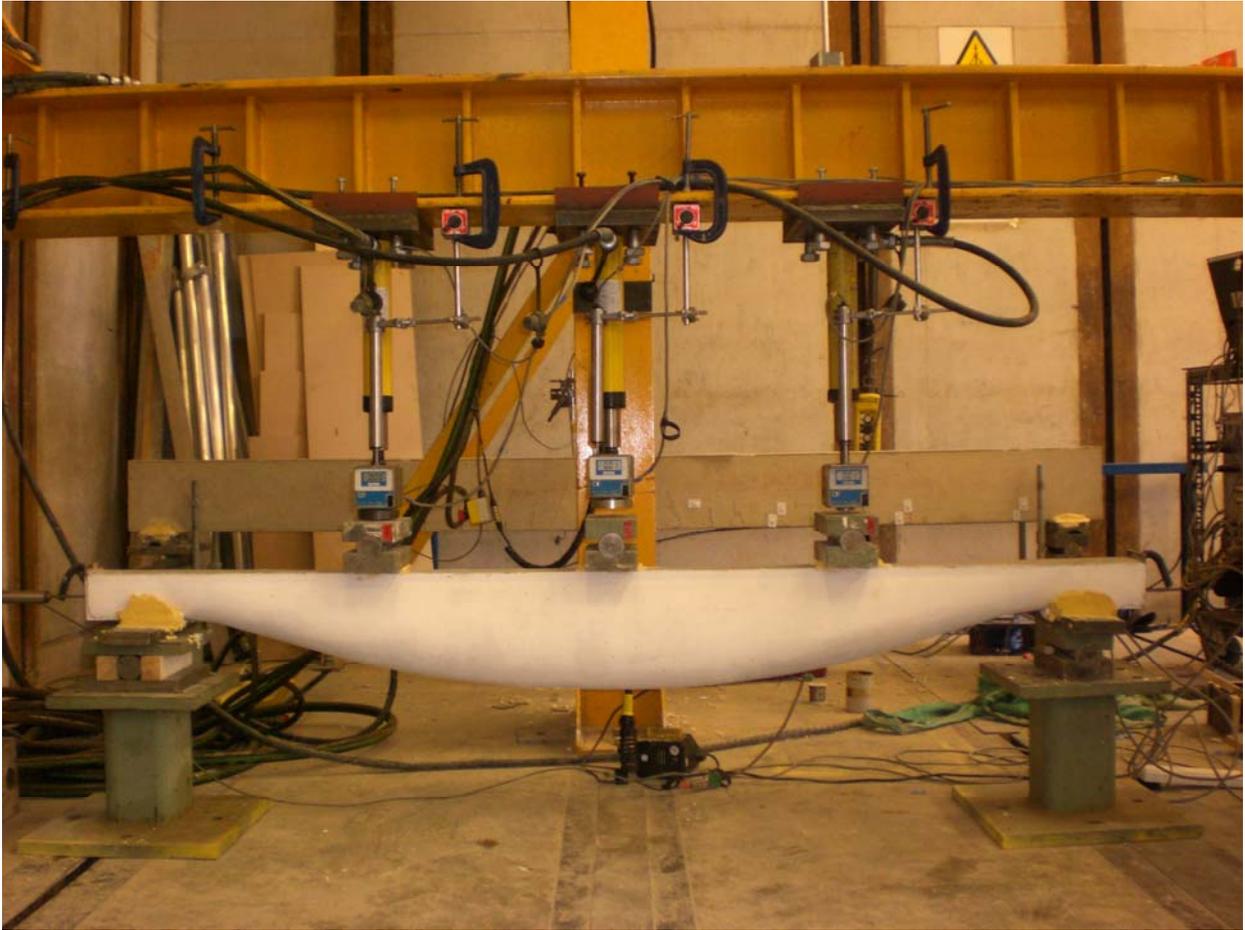
Figure 7: Test set-up
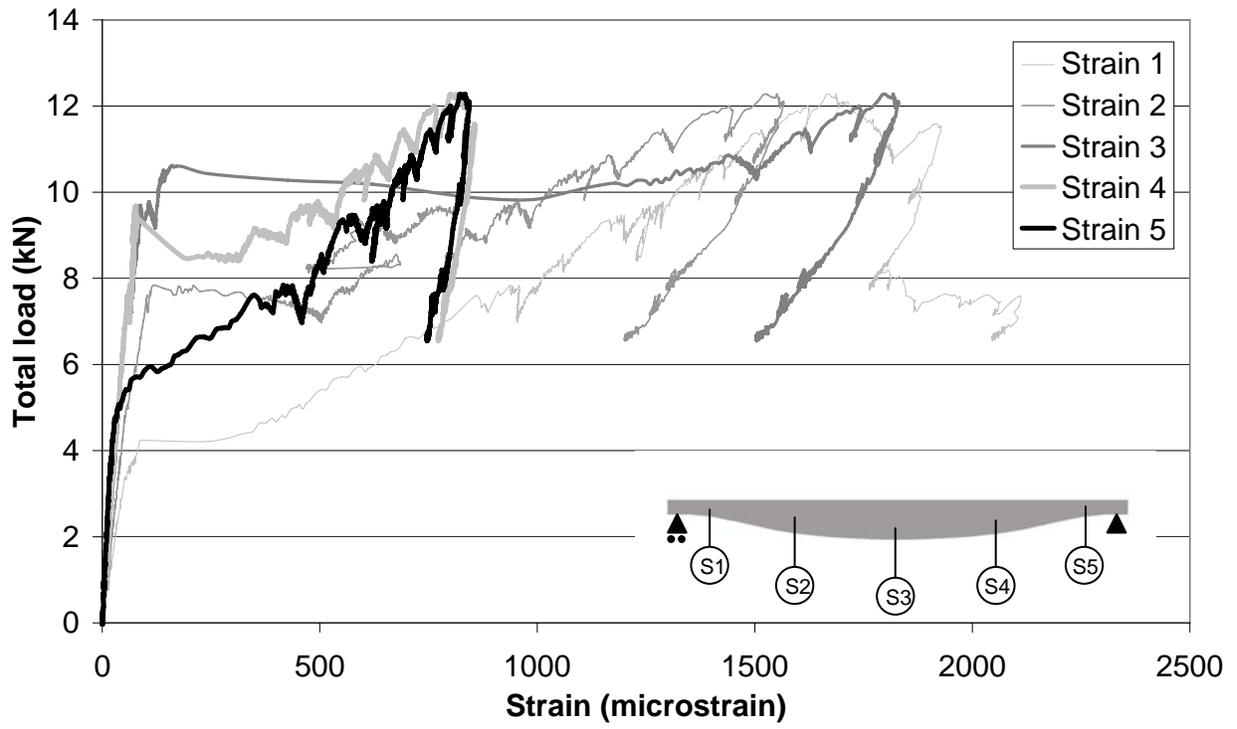
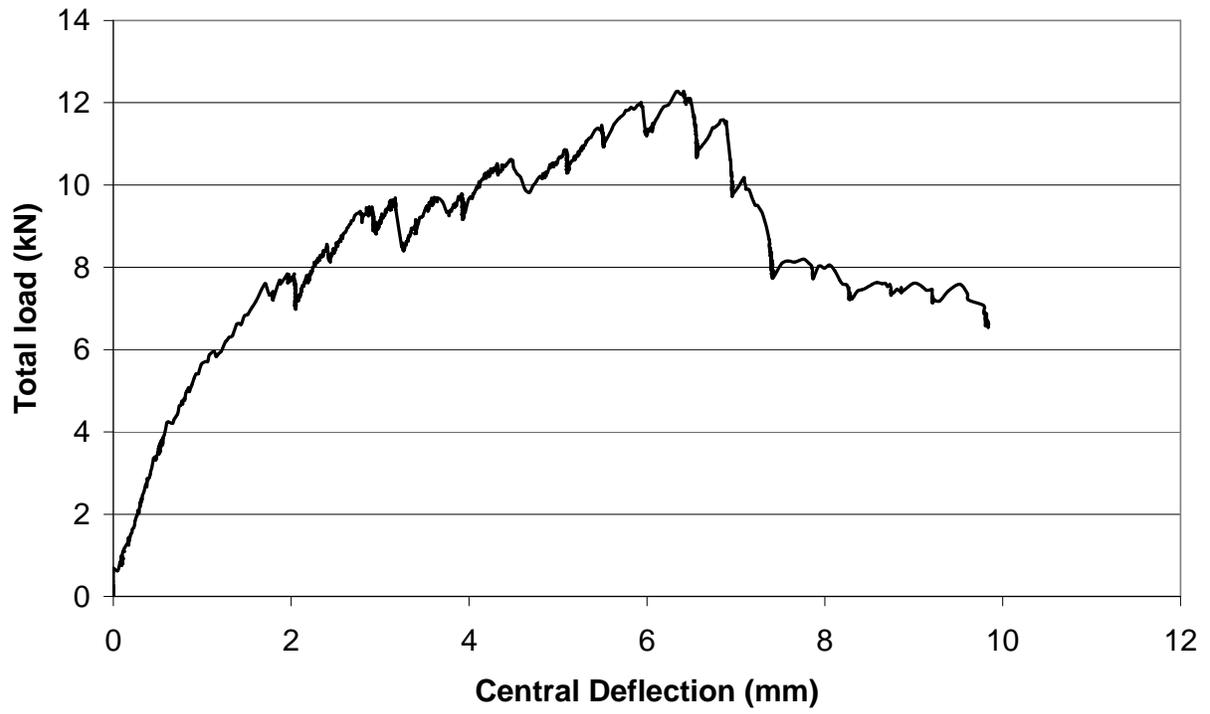Figure 8: Beam 1 - Load versus steel reinforcement strains
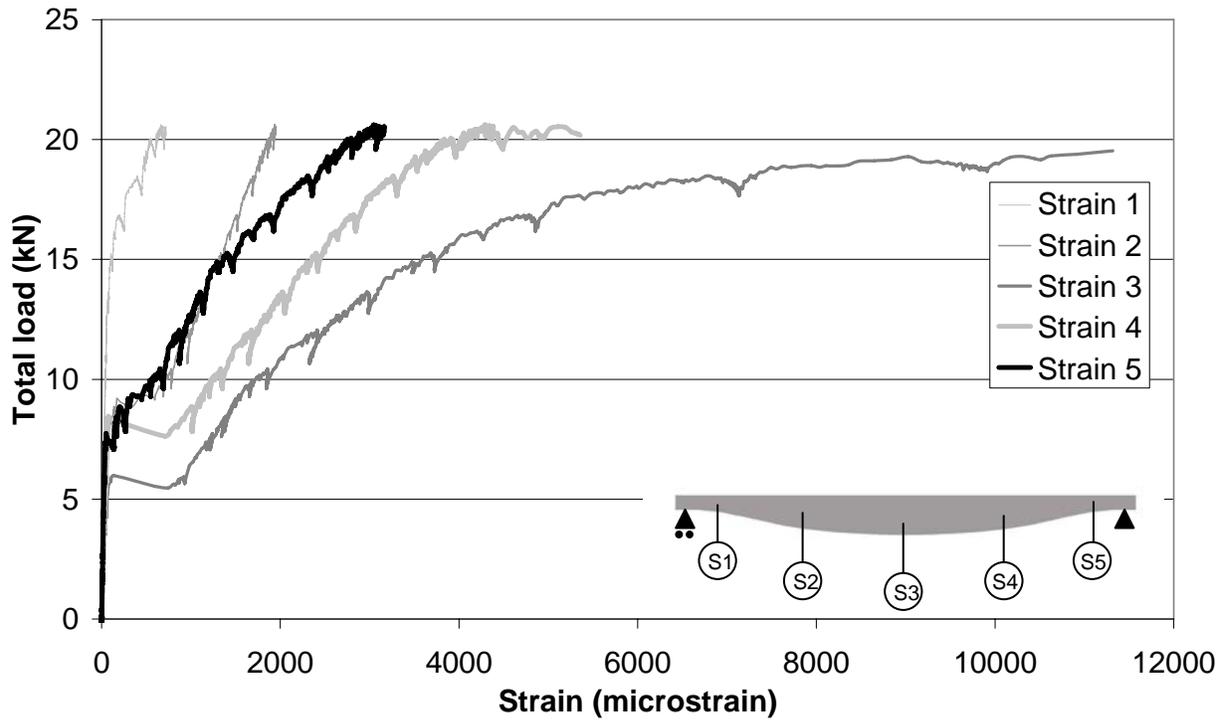
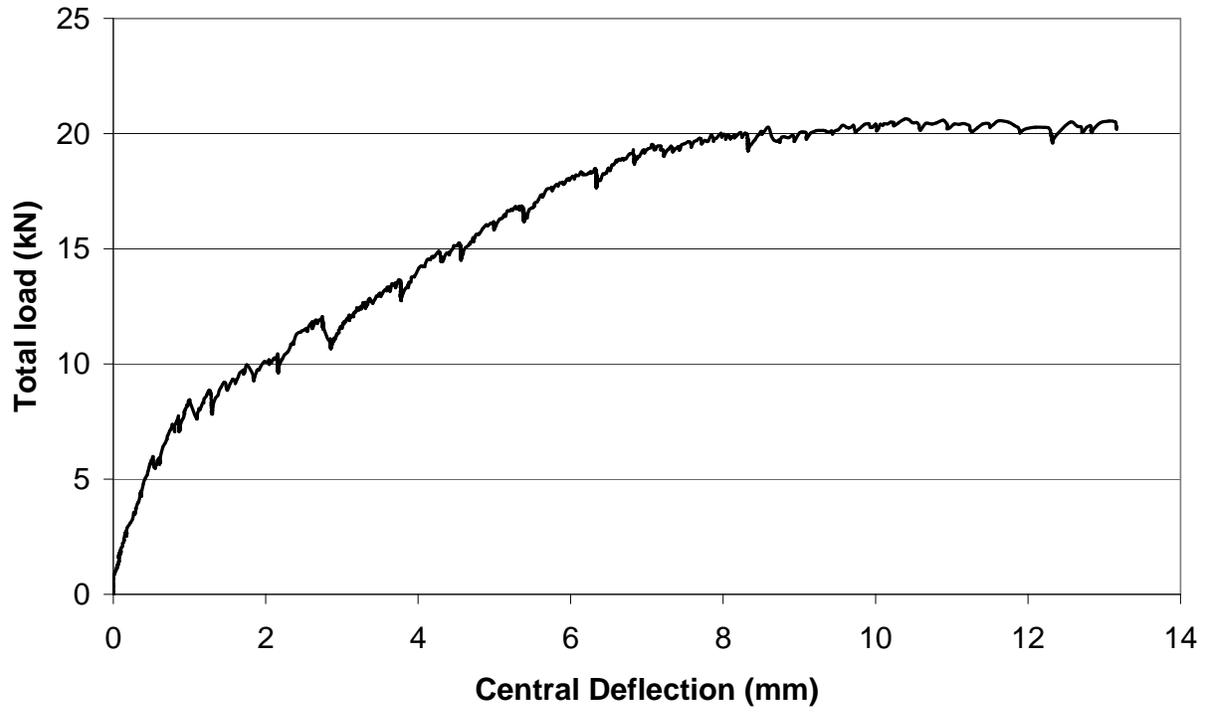Figure 9: Beam 1 - Load versus deflection

Figure 10: Beam 2 – Load versus steel reinforcement strains

Figure 11: Beam 2 - Load versus deflection